Hindawi
Geofluids
Volume 2023, Article ID 8910226, 10 pages
https://doi.org/10.1155/2023/8910226

Research Article

Experimental Study on Freezing Strength of Soil-Concrete Lining Interface in Cold Regions

Zhang Fuping,[1,2] **Shang Jianguo**,[1,2] **Geng Wenting**,[1,2] **and He Pengfei**[1,3]

[1]*State Grid Gansu Electric Power Company Construction Branch, Lanzhou 730050, China*
[2]*State Grid Gansu Electric Power Company, Lanzhou 730030, China*
[3]*Lanzhou University of Technology, Lanzhou 730050, China*

Correspondence should be addressed to Zhang Fuping; 13993128806@163.com and He Pengfei; hepf@lut.edu.cn

Received 21 July 2022; Revised 24 March 2023; Accepted 10 April 2023; Published 27 April 2023

Academic Editor: Mohammed Fattah

The lining of water conveyance canals in cold regions is usually subjected to serious damage, such as spalling, bulging, and fracture, due to the harsh natural environment. The main causes of these types of damage are the normal frost-heaving force and tangential frost-heaving force (adfreeze force) acting on the liner plate. In this study, the adfreeze forces between the foundation soil and liner plate were studied using the direct shear test, considering the effects of the initial water content, test temperature, and compactness. The results show that the increase of the water content, the increase of the temperature, and the decrease of the compactness increased the interfacial peak shear displacement, and they all varied in the range of 0.3–1.6 mm. With the decrease of the initial water content of the soil sample, the increase of the test temperature, and the decrease of the compactness, the peak shear stress decreased significantly with the amplitude between 51 and 87%. The interfacial cohesion decreased significantly with the increase of the initial water content, the increase of the temperature, and the decrease of the compactness. The interfacial friction angle had no apparent variation pattern. At room temperature, the interfacial friction angle decreased significantly with the increase of the water content. When the water content was 30%, the interfacial friction angle was almost lost completely, which can easily lead to the sliding loss of the foundation soil and further damage, such as the instability of the lining.

1. Introduction

Permafrost and seasonally frozen soil accounts for about 25% of the world's land area [1]. Due to the volume expansion of the water in the soil pores after freezing and the moisture migration along capillaries under the action of the temperature gradient which forms ice lenses, constructions on the frozen ground regions are often damaged by frost heave [2–5]. For water conveyance canals built in frozen soil areas, if the leakage water in the canal foundation soil cannot be drained after the water is stopped, the gradual freezing of the soil during winter will cause severe frost-heaving damage, and sometimes, the maximum frost-heaving amount can reach 15 cm [6, 7]. In addition, in the spring, ice thawing increases the water content of the foundation soil, and the decrease in soil strength and carrying capacity can easily cause damage, such as canal-slope-sliding collapse [8]. For example, in the irrigated area of Chahar in Heilongjiang Province, 83% of the water conveyance canals suffered frost-heaving damage [9]. Of the 216 major water conservancy projects in Jilin Province, 39.4% suffered frost-heaving damage [10]. In the canals of some irrigation areas in Shaanxi Province, the crack rate of the concrete impermeable board on the shady slope is 75.5% and that of the sunny slope is 27% under frost-heaving effects, causing a large waste of water resources [11]. Located in the Altay Prefecture, the Northern Xinjiang Water Transfer Project has provided abundant water resources for Urumqi and the residents and factories along the route since its completion, which has promoted local economic and social development. However, the climatic environment and geological conditions along the canal are complex and variable, with the extreme maximum temperature reaching 40.5°C and extreme minimum temperature reaching

-41.5°C. This makes the lining subject to frequent frost damage, such as spalling, bulging, and sliding collapse, under external loads, such as excessive frost-heaving force. The frost damage issue in canals has seriously affected the effectiveness of various water conveyance projects and wasted valuable water resources [12].

Frost damage phenomena in canals manifest through several aspects, including lining damage, impermeable layer damage, joint material shedding, foundation soil collapse, and ice jamming [13]. The most serious among them is the lining damage which is mainly caused by the uneven frost-heaving effects of the foundation soil in the canal bed [14]. Due to the influence of leakage, rainfall, and groundwater level, the free water in the canal foundation soil is unevenly distributed along the depth direction; the frost heave of the soil body during freezing imposes an uneven load on the lining, coupled with the freezing effect; the concrete lining and the contact soil freeze as one and are also subjected to the restraining effect between the bridle path, the bottom plate, and the slope plate. The greater the free frost-heaving amount of the soil body, the greater the force exerted on the lining; the more uneven the frost heave, the more uneven the force exerted on the lining. However, the lining material has low elasticity and tensile strength. When the freezing force and frost-heaving force are large enough, the lining structure is bound to be damaged, leading to increased leakage [15]. Under the repeated action of freezing and thawing cycles, the accumulated development of the frost-heaving deformation of the foundation soil causes more and more serious damage on the lining structure. To establish a simple and practical mechanical model for frost-heaving damage of the lining structure, Wang et al. [14–17] analyzed the form and characteristics of frost-heaving damage of the concrete lining of canals, which produced uneven frost-heaving deformation of different directions and sizes, due to the difference of physical properties of soil bodies at different locations of the canal slope foundation soil. Under the action of the frost-heaving force, freezing force, and restraining force, the lining plate strength or stiffness fails and spalling occurs, which causes leakage and increases the water content in the foundation soil, and the long-term effect leads to more and more serious lining damage [14]. Through the analysis of forces over the lining, it is found that the freezing force, frost-heaving force, and restraining force are interdependent and can eventually be expressed as a function of the maximum tangential freezing force [14]. Therefore, to analyze the damage mechanism of the lining plate in depth, it is necessary to carry out an in-depth study on the characteristics of the freezing-force variation between the lining plate and the foundation soil.

Scholars have conducted a lot of research on the mechanical properties of the interface between constructions and the frozen ground. Bondarenko and Sadovskii [18] studied the effect of temperature on freezing strength and obtained the empirical freezing-strength calculation formula. Biggar and Sego [19] conducted experimental studies on the instantaneous freezing strength and long-term freezing strength of the interface between the rock and frozen ground, and the results showed that the temperature has a big influence on the interfacial cohesion but a small influence on the interfacial friction angle. Ladanyi [20] tested the freezing strength of the perfusion pile and frozen ground. The result showed that the salt content and temperature of the frozen ground caused variation in the unfrozen water content in the frozen ground around the pile base, which in turn affected the freezing strength. Ji et al. [21] studied the freezing strength of the interface between the sand and aluminum. The result showed that the controlling factor changed from the internal friction angle to the cohesion as the temperature decreased. Wen et al. [22] tested the freezing strength at the interface between the cast-in-place concrete and frozen ground, showing that the hydration heat changed the interfacial roughness, which in turn affected the interfacial freezing strength. Chen et al. [23] did shear tests at the interface between the frozen ground and concrete and fiberglass, showing that the interfacial freezing strength increased as the test temperature decreased, and the initial water content of the soil body increased. Shi et al. [24] determined the freezing strength of the contact surface of the frozen ground and steel pipe using the pile-pressing method, and the results showed that the contact surface temperature had significant effects on the surface roughness. Sun et al. [25] carried out the orthogonal direct shear tests on the contact surface of the frozen ground and steel plate, and the results showed that the water content of the soil body had the greatest effect on the freezing strength. Sun et al. [26] studied the freezing strength of the interface between the frozen ground and the structures under different conditions, showing that the interfacial freezing strength is affected by the freezing temperature, normal stress, properties of the frozen ground, roughness of the contact surface, and so on. Wang et al. [27, 28] redefined the roughness of the stainless-steel plate under different roughness conditions and conducted experimental studies on the freezing strength of its interface with the frozen ground.

In summary, the freezing-force variation characteristics between the canal lining plate and foundation soil in cold regions are the key to affect its force analysis and damage mechanism analysis, while the interfacial freezing strength is influenced by the physical properties of the soil, temperature, water content, compactness, shear rate, and other factors. However, the physical and mechanical properties of the soil body under different geological conditions are very different. To better serve the prevention and control of Northern Xinjiang water conveyance canal disasters, this paper selected two typical canal bed foundation soil samples, conducting experimental research on the interfacial freezing strength and its parameter variations under different initial amounts of water content, test temperatures, and degrees of compactness, and analyzing the variation of the maximum bending moment in the lining plate at different freezing strengths. The research results are expected to provide scientific references for the controlling of water conveyance canal disasters.

2. Experimental Materials and Methods

2.1. Experimental Materials. The soil samples used in the tests were taken from the Northern Xinjiang water conveyance canal, and the collection area has a continental climate with hot summers and cold winters. Both soil samples are expansive soils, which present a lighter color of red (Figure 1(a)) and green (Figure 1(b)) and are therefore named CH-R and CL-G, respectively. Their physical properties were tested according to the "Standard for Engineering Classification of Soil" [28], and the physical indices are shown in Table 1, while the particle size distribution of the test soil samples is shown in Figure 2.

During the direct shear test, the lining specimens were too small to be made with standard concrete, so the larger particles in the sand were eliminated. The lining specimens for the test were made with cement mortar, called mortar blocks. In the whole test process, the shear characteristics of the interface between the mortar block and soil body were mainly studied, while the strength of the mortar block itself had little effect on the interfacial shear characteristics. No obvious abrasion or sand flaking was found on the surface of the mortar block during the test, so the shear characteristics of the interface between the mortar block and soil sample can be an approximate substitute for that of the interface between the concrete lining and soil body in actual engineering. The preparation of specimens in the whole test included mortar block specimen preparation, soil sample preparation, and frozen soil-mortar block specimen preparation [23]. Among them, the mortar block specimen preparation process consisted of five steps: (1) A cutting ring of 61.8 mm diameter and 20 mm height was used as a mold, and a layer of Vaseline was evenly applied to the inner wall of the cutting ring. (2) The cement mortar was made of PO32.5 ordinary silicate cement mixing with natural river sand; the ratio of the cement, sand, and water was 1.8 : 3 : 1. Due to the small size of the specimen, the large particles, such as gravel, in the mortar were eliminated to ensure that the specimen size could reach more than 5 times the particle size. (3) The cement mortar was filled evenly into the cutting ring; then, it was subjected to vibration and smoothening to make the thickness of the specimen the same as the height of the cutting ring. (4) The finished mortar block specimens were maintained for 28 days according to the standard procedure. (5) A jack was used to eject the mortar block specimens from the cutting ring, the thickness of the specimens was measured, and those that were 20 mm thick were selected as the final mortar block specimens. All mortar block specimens were made simultaneously with similar degrees of surface roughness, and they looked relatively rough when observed with the naked eye. During the process of soil sample preparation, first, the original soil material was dried naturally and mixed thoroughly, then crushed and filtered through a 2 mm sieve, and the initial water content was measured via the drying method; then, the soil sample was prepared according to the predetermined water content. After completion, the soil samples were put into sealed bags for 24 h to uniformly distribute the water content, and the water content of the soil sample was measured as the actual water content. Since the differences between the actual water content and the predetermined water content were all within 0.3%, the designed water content was used to analyze the test data.

Figure 1: Pictures of two expensive soils.

The frozen soil-mortar block specimen was prepared in four steps using a 40 mm high, 61.8 mm inner diameter cutting ring as the specimen bin: (1) One end of the bin was sealed with plastic tape, and the mortar block specimen was placed in the bin near the plastic tape side. (2) According to the predetermined dry density and water content of the soil sample, a certain mass of wet soil was weighed and loaded into the specimen bin evenly. (3) The standard sample press developed by the State Key Laboratory of Frozen Soil Engineering was used to slowly and uniformly apply pressure to the soil sample loaded into the specimen bin until the height of the soil sample reached 20 mm, and the dry density of the soil body in the specimen bin was determined according to the predetermined value. (4) The whole specimen bin was wrapped with cling film to prevent moisture loss, and then, it was frozen rapidly at -25°C for 24 h. After the sample was completely frozen, the frozen soil-mortar block specimen was jacked out from the specimen bin to obtain the test sample. Figure 3 shows the frozen soil-mortar block interfacial shear test specimen of the red soil under the unfrozen condition.

2.2. Experimental Methods. The shear strength test at the frozen soil-mortar block interface was carried out using a ZJ quadruple strain-controlled direct shear instrument manufactured by the Nanjing Soil Instrument Factory Limited Company. The shear box was composed of two parts, upper and lower, with the same height of 20 mm. The interface between the upper and lower boxes was the shear surface, and the contact surface of the frozen soil-mortar block test sample coincided with the shear surface. The direct shear instrument can automatically record the horizontal displacement of the shear box and the interfacial shear force. The test was conducted at the low-temperature laboratory of the State Key Laboratory of Frozen Soil Engineering, where the ambient temperature can be automatically controlled with an accuracy of ±0.5°C. The ambient temperature was measured and adjusted in real time during the test to ensure that the ambient temperature would be as close as possible to the predetermined test temperature.

After the sample was completed with rapid freezing, the test process of the interfacial freezing strength includes the following: (1) According to the predetermined test temperature, the temperature was maintained via the thermostat for 24 h to ensure that the whole sample was in a stable temperature state. (2) The connection status of the test instrument and the controlling computer was checked to make sure the

Table 1: Basic properties of soils.

No.	Soil classification	LL (%)	PL (%)	Gs	w_{opt} (%)	ρ_{d-max} (g·cm^3)	FS (%)
CL-G	Low-liquid-limit clay	46.9	23.5	2.69	19.1	1.71	76
CH-R	High-liquid-limit clay	57.6	26.8	2.7	21.8	1.67	90

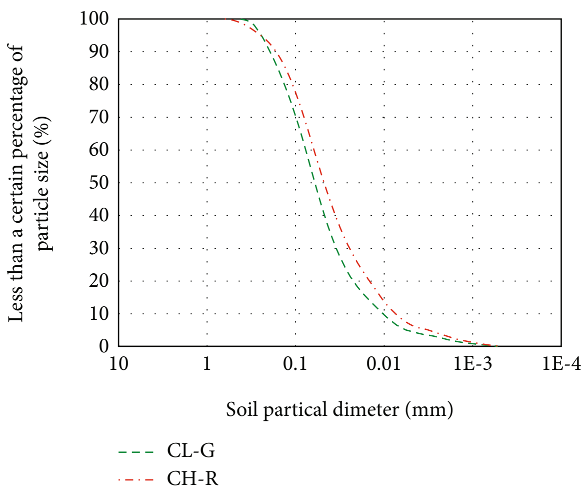

Figure 2: Distribution curves of soil particles.

Figure 3: Red soil-mortar plate interfacial sample at unfrozen condition.

controlling software was running normally. (3) The thermostat sample was quickly and carefully loaded into the shear box to ensure that the interfacial contact state and temperature were minimally disturbed. (4) Shearing was started, with the computer automatically recording the shear displacement and shear stress.

During the test, the normal stress was controlled to be 50, 100, 200, and 300 kPa. The canal foundation soil will have a relatively large variation of water content due to leakage and other factors. The initial water content of the soil sample in the test was set as 10, 14, 18, 22, 26, and 30%. The test temperature was set as 19, -1, -3, -5, and -8°C. The repeated freezing and thawing in alpine regions may cause variations in soil composition and dry density, and the effects of different degrees of compactness on the interfacial freezing strength were considered in the test, with compactness at 75, 80, 85, 90, and 95%. In fast shear tests with a shear rate of 0.8 mm/min, the specimens could be sheared within 10 min, thus ensuring that the effects of temperature fluctuations in the low-temperature laboratory on the internal temperature of the specimens could be neglected.

3. Test Results

3.1. Shear Stress-Shear Displacement Relationship. Since the quantity and quality of the initial composition of the soil body at the interfacial shear band and the cemented ice are different under different test temperatures, initial amounts of water content, and degrees of compactness, the interfacial shear stress-shear displacement relationship also shows different variation laws. This subsection analyzes the variation laws of the freezing strength at the interface of the red soil body and mortar block; the green soil body had a similar change law and is not repeated here.

Figure 4 shows the effects of different amounts of water content on the shear displacement of the interfacial shear stress (normal stress of 100 kPa, temperature of -5°C, and compactness of 95%). It can be seen that the curve pattern varies significantly as the water content decreases. The peak intensity is 768 kPa at the initial water content of 30%, and the curve exhibits an obvious strain-softening-type characteristic. After the shear stress reaches its maximum value, the shear stress decreases rapidly until it reaches a residual state due to the brittle failure of the interfacial cemented ice [26–28]. The peak strength is 142 kPa at the initial water content of 14%, at which time the curve pattern exhibits a weak-softening characteristic. The peak shear stress decreases due to the interfacial cemented ice content, and within, the shear band of the soil body decreases after the water content is reduced. The interfacial peak shear stress is 98 kPa at the initial water content of 10%, which is 87% lower than at the initial water content of 30%. In contrast, the interfacial peak strength under nonfreezing conditions is 82 kPa, indicating that the interfacial cemented ice content is very low at an initial water content of 10%. The interfacial peak displacement also shows a gradual decrease with decreasing initial water content, from 1.6 mm at the water content of 30% to 0.7 mm at the water content of 10%, because, as the water content increases, the interfacial cemented ice content, the interfacial shear strength, and the corresponding plastic shear deformation also increase [29, 30].

Figure 5 shows the effects under different test temperatures on the interfacial shear stress-shear displacement relationship (initial water content of 18%, normal stress of 100 kPa, and compactness of 95%). It can be seen that the interfacial curves show an obvious strain-softening type at

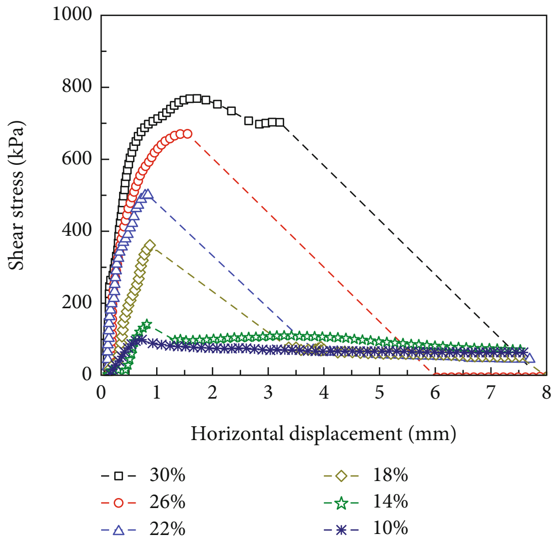

Figure 4: Shear stress vs. horizontal displacement of frozen red soil-concrete interface under different amounts of initial water content (temperature of -5°C, normal stress of 100 kPa, and compactness of 95%).

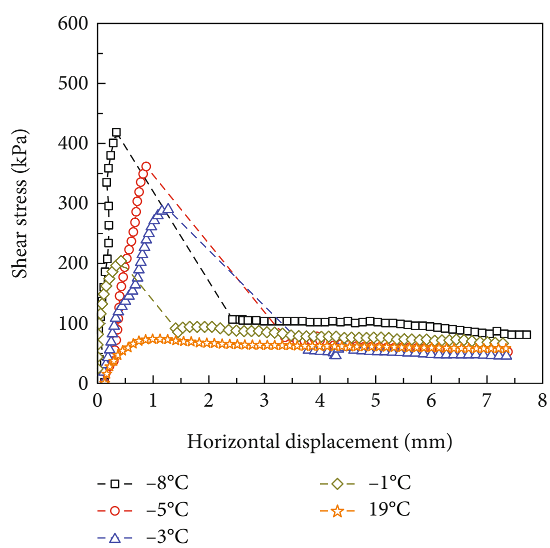

Figure 5: Shear stress vs. horizontal displacement of frozen red soil-concrete interface under different temperatures (initial water content of 18%, normal stress of 100 kPa, and compactness of 95%).

negative temperature conditions and a strain-hardening type at positive temperature conditions. This is because the content of cemented ice in the soil body increases with decreasing temperature [30–32]. For the strain-hardening curve, including prepeak and residual stages. Such a curve often appears at the interface between the soil and structure in unfrozen conditions. At the frozen state, the strain-softening curve can be divided into the prepeak, postpeak, and residual stages. In the prepeak stage, the interface remains intact with the increase of shear force, and the shear zone undergoes elastic deformation. Subsequently, with the growth of shear displacement, the part of the interface cement with less strength starts to be gradually destroyed.

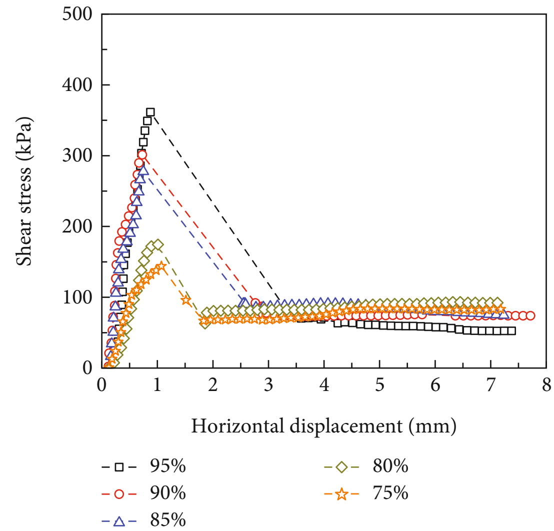

Figure 6: Shear stress vs. horizontal displacement of frozen red soil-concrete interface under different degrees of compactness (initial water content of 18%, normal stress of 100 kPa, and temperature of -5°C).

In contrast, the contact surface of the destroyed part gradually establishes friction, which replenishes part of the strength lost due to the destruction of the cement, which shows a nonlinear growth of the shear stress curve at the macroscopic level until the maximum shear stress. The maximum shear stress is the equilibrium point between the interfacial cementation strength and friction strength, before which the cementation strength dominates. In the postpeak stage, the cement band fracture gradually increases as the relative displacement continues to rise. At this time, the percentage of fracture interface of the cemented zone far exceeds that of the intact interface. It gradually approaches complete fracture, and the frictional strength generated in the fracture region of the cemented body is no longer sufficient to replenish the strength lost by the fracture of the cemented body. It is expressed in the macroscopic shear stress curve as the shear stress decreases. In the residual stage, after the interfacial cementation body is completely fractured, the interfacial strength is completely provided by the friction force, manifested macroscopically as the shear stress curve becomes horizontal because the contact state of the interface no longer changes significantly. The interfacial peak strength decreases from 418 kPa at -8°C to 74 kPa at 19°C, which is a decrease of 82% of the peak strength. The variations of the residual strength at different test temperatures are small compared to those of the peak strength because the interfacial cemented ice is damaged in the residual phase, and the temperature has less effect on the interfacial friction force [33, 34]. The variation pattern of the interfacial peak displacement is not obvious and between 0.3 and 1.3 mm overall.

Figure 6 shows the effects of different degrees of compactness on the interfacial shear stress-shear displacement (initial water content of 18%, temperature of -5°C, and normal stress of 100 kPa). The curves are all strain-softening under different degrees of compactness. The peak strength

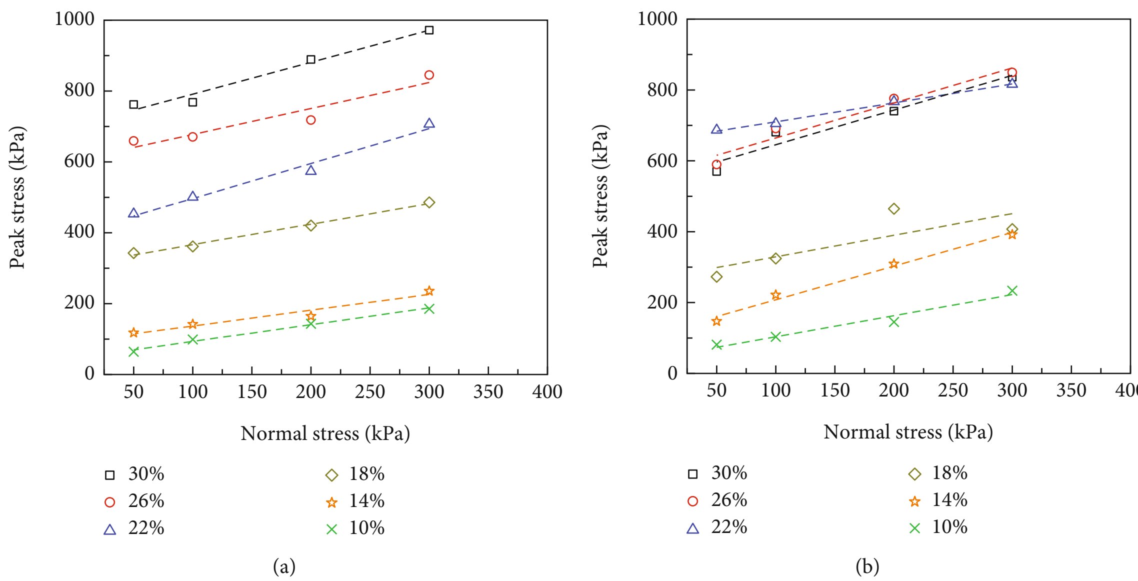

Figure 7: Peak shear stress vs. normal stress under different initial amounts of water content (temperature of -5°C and compactness of 95%). (a) Red soil; (b) green soil.

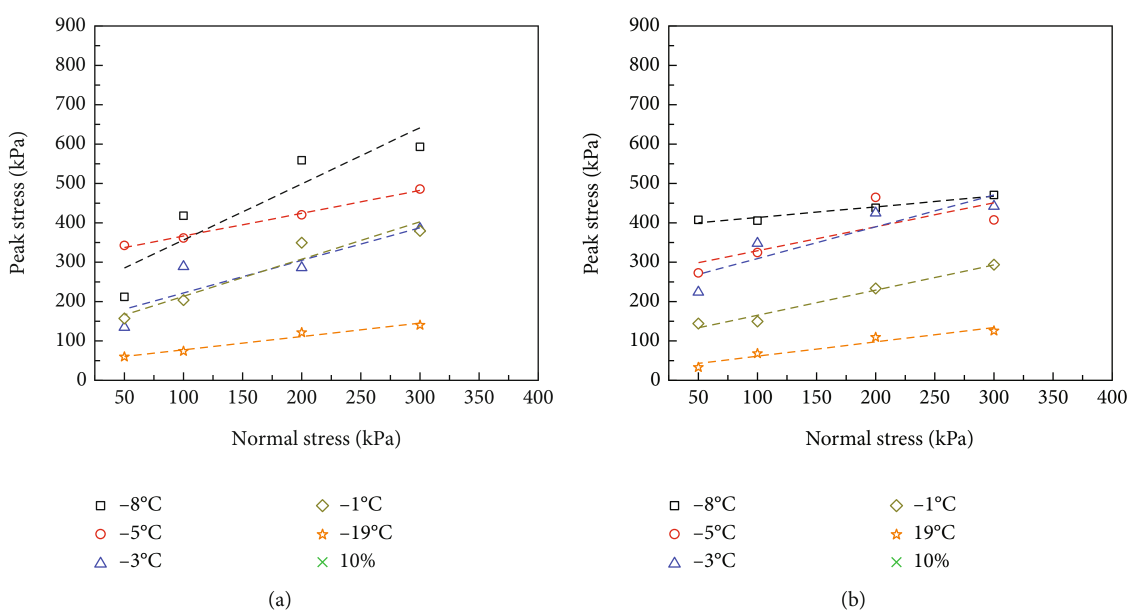

Figure 8: Peak shear stress vs. normal stress under different temperatures (initial water content of 18% and compactness of 95%). (a) Red soil; (b) green soil.

gradually decreases as the compactness decreases, from 361 kPa at compactness of 95% to 144 kPa at compactness of 60% to 75%. The main reason is that when the compactness decreases, the spacing between soil particles within the soil skeleton increases, and the cohesion and occlusion between particles decrease, while the effective contact area between the interfacial soil particles and the concrete surface decreases, which makes the interfacial shear strength decrease [5, 34, 35]. It can also be seen that the variation pattern of the peak shear displacement is not obvious and fluctuates between 0.7 and 1.1 mm.

3.2. Interfacial Strength. Figure 7 shows the effects of different amounts of water content on the interfacial peak shear stress (temperature of -5°C and compactness of 95%). From Figure 7(a), it can be seen that the interfacial peak strength decreases significantly with decreasing water content at different normal stresses. The reason is the variations of cemented ice content within the soil body at different amounts of water content [30, 34]. Under a normal stress of 300 kPa, the peak stress decreases from 972 kPa at water content of 30% to 186 kPa at water content of 10%, which is a decrease of 81%. From Figure 7(b), it can be seen that

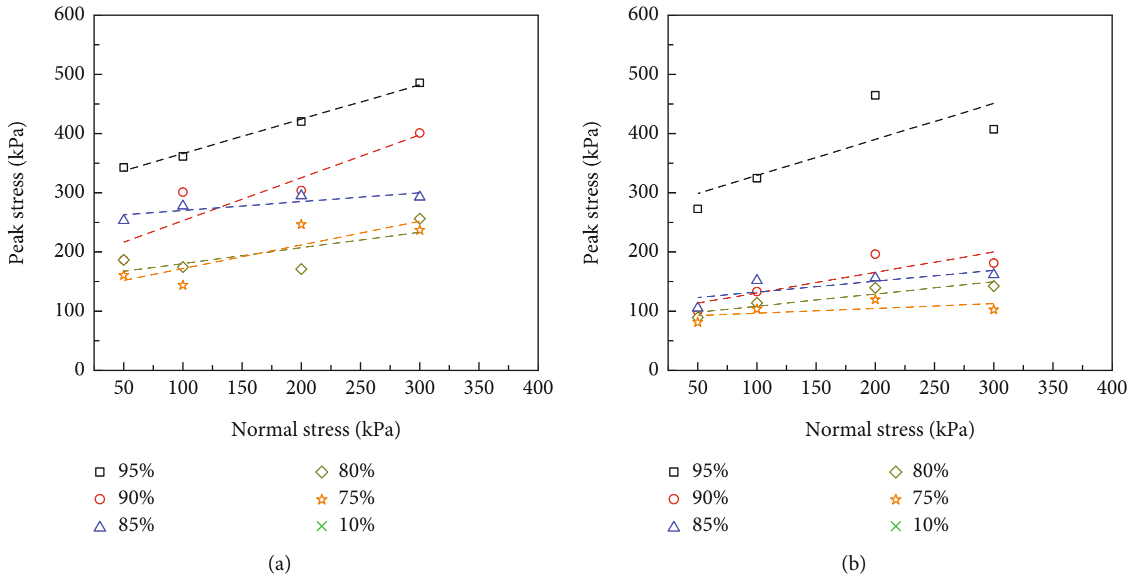

FIGURE 9: Peak shear stress vs. normal stress under different degrees of compactness (initial water content of 18% and temperature of -5°C). (a) Red soil; (b) green soil.

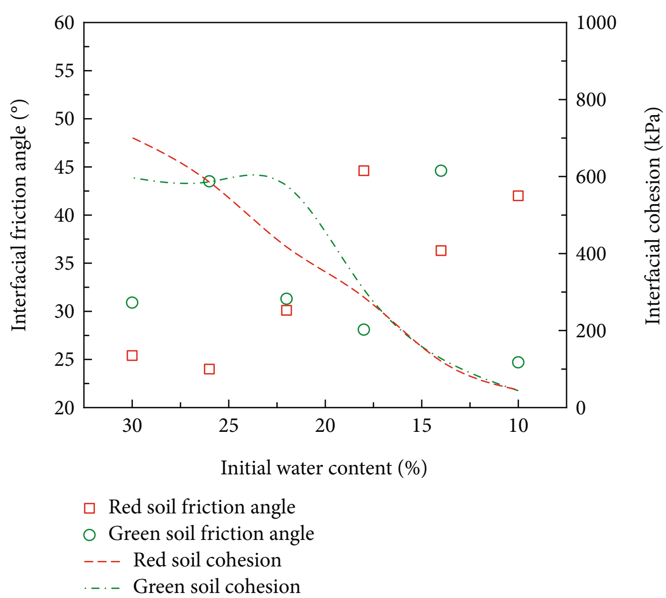

FIGURE 10: Influence of initial water content on interfacial friction angle and cohesion (temperature of -5°C and compactness of 95%).

the variations of the peak stress at the water content of 30%, 26%, and 22% are not obvious, but when the water content decreases further, the peak stress shows a significant decrease. The interfacial peak stress of red soil is slightly higher than that of the green soil at the same water content, presumably due to the different physical properties, such as the liquid-plastic limits of the two soil materials.

Figure 8 shows the effects of different test temperatures on the interfacial peak stress. The overall analysis shows that as the test temperature increases, the cemented ice content in the soil body decreases so that the interfacial peak stress decreases gradually, as shown in Figure 8(a) when, at a normal stress of 300 kPa, the peak shear stress decreases from 593 kPa at -8°C to 140 kPa at 19°C, which is a decrease of 76%. Compared with the peak stress which decreases rapidly as the water content decreases in Figure 7, the reason for the peak stress decreasing slowly as the temperature increases in Figure 8 is that the cemented ice content is low in the soil body during freezing when the water content is 18% in the test condition in Figure 8.

Figure 9 shows the effects of different degrees of compactness on the interfacial peak shear stress. From Figure 9(a), it can be seen that the peak shear stress gradually decreases with decreasing compactness, because at the same water content and temperature, the decrease in compactness means that the internal skeletal structure of the soil body becomes looser and the interparticle cohesion and occlusion are weakened, while the effective contact area between the

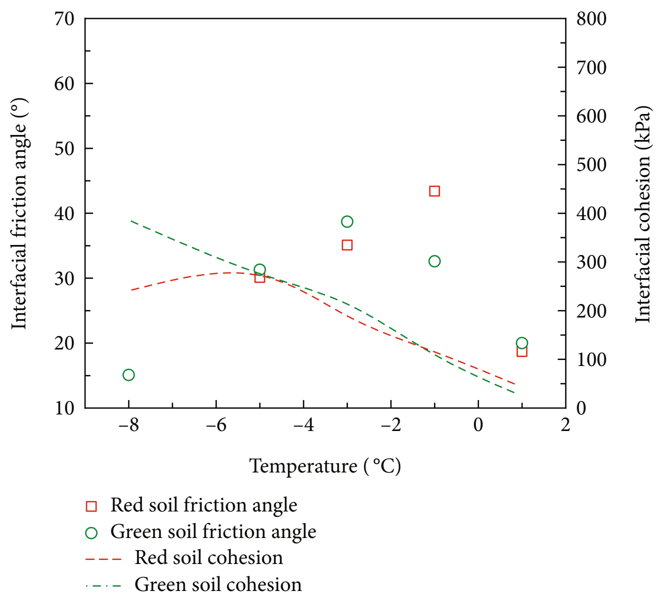

Figure 11: Influence of temperature on interfacial friction angle and cohesion (initial water content of 18% and compactness of 95%).

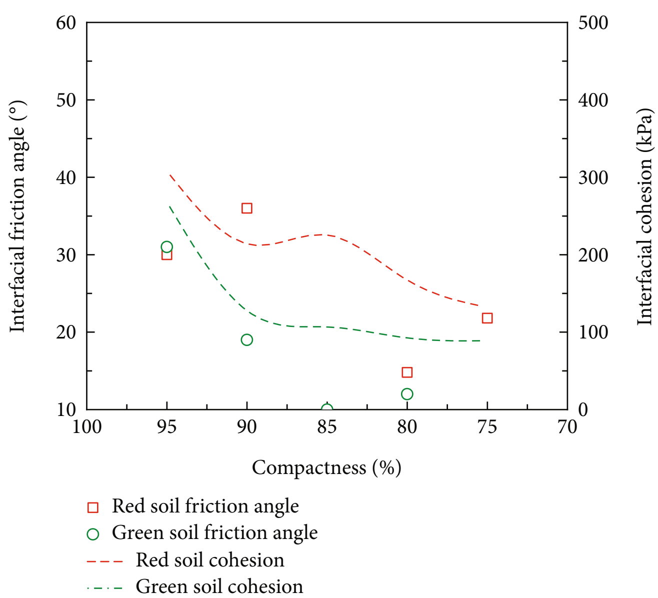

Figure 12: Influence of compactness on interfacial friction angle and cohesion (initial water content of 18% and temperature of -5°C).

interfacial soil body and the mortar block decreases [5, 34]. For example, at a normal stress of 300 kPa, the peak shear stress decreases from 486 kPa at compactness of 95% to 237 kPa at compactness at 75%, which is a decrease of 51%. From Figure 9(b), it can be seen that the peak shear stress decreases significantly when the compactness decreases from 95% to 90%, and then it decreases slowly as the compactness decreases. At the same compactness value, the interfacial peak shear stress of the green soil is lower than that of the red soil.

3.3. Interfacial Strength Parameters. Mohr-Coulomb criterion was used to analyze the interfacial peak shear stresses at different normal stresses and to calculate the interfacial friction angle and cohesion. Figure 10 shows the effects of different amounts of water content on the interfacial friction angle and cohesion. It can be seen that at different amounts of water content, there is no obvious variation in the interfacial friction angle, while the interfacial cohesion decreases significantly with the decrease of water content; for example, the water content decreases from 30% to 10%, and the cohesion of the green clay decreases from 597 kPa to 44 kPa, which is a decrease of 93%. Figure 11 shows the effects of different temperatures on the interfacial friction angle and cohesion. It can be seen that the interfacial friction angle still has no obvious variation pattern, while the interfacial cohesion shows an obvious decrease with the increase of the temperature. For example, the cohesion of the green clay drops from 386 kPa at -8°C to 25 kPa at 19°C, which is a decrease of 94%. This is because the interfacial cohesion is mainly provided by the cemented ice, and with the increase of the temperature and the decrease of the initial water content, the content and quality of the interfacial cemented ice will show a great decrease, which leads to the decrease of the interfacial cohesion. While the interfacial friction angle is mainly provided by the friction between the soil body and the mortar block, the temperature and water content have less effect on the interfacial friction [34]. Figure 12 shows the effects of different degrees of compactness on the interfacial friction angle and cohesion, and it can be seen that as the compactness decreases, both the interfacial cohesion and friction angle show a decreasing trend, which is consistent with the analytical conclusions in the previous section.

4. Conclusion

The freezing strength of the interface between the subsoil and mortar block of the northern border water transmission canal was investigated using a series of direct shear tests. The shear behavior between the concrete lining and the foundation soil was approximated using the shear behavior of the interface between the cement mortar block and the soil body, considering the effects of different test temperatures, the initial water content of the soil body, and the compactness. The following conclusions were obtained by analyzing the variation of shear properties of the interface between red soil and mortar block:

(1) The interfacial peak shear displacement increases gradually with the increase of the water content, the increase of the temperature, and the decrease of the compactness, but it always varies in the range of 0.3–1.6 mm

(2) The interfacial peak stress varies significantly under different test conditions. The peak stress decreased by 81% when the initial water content of the soil body decreased from 30% to 10% (test temperature of -5°C and compactness of 95%); the peak stress decreased by 76% when the test temperature increased from -8°C to 19°C (initial water content of 18% and compactness of 95%). When the compactness decreased from 95% to 75% (initial water content of 18% and test temperature of -5°C), the peak stress decreased by 51%

(3) With the increase of the initial water content, the increase of the temperature, and the decrease of the compactness, the interfacial cohesion decreases obviously, and the interfacial friction angle has no obvious variation pattern

Data Availability

The data used to support the findings of this study are included within the article.

Additional Points

Highlights. Investigate the freezing strength of two special frozen-soil-lining interfaces. Focus on both shear behavior and displacement characteristics under different conditions. Present key parameters for the case of the interface shear behavior.

Conflicts of Interest

The authors declare no conflict of interest.

Authors' Contributions

Fuping Zhang was responsible for the lab design and project administration. Jianguo Shang was responsible for the lab testing, formal analysis, and original draft. Wenting Geng was responsible for the data curation and formal analysis. Pengfei He was responsible for writing of the original draft preparation and formal analysis.

Acknowledgments

This work was supported by the Natural Science Foundation of Gansu Province (nos. 22JR5RA308 and 21YF5GA041) and State Grid Gansu Electric Power Company Science and Technology Project (no. SGGSJS00XMYBJS2100062).

References

[1] Y. Zhou, D. Guo, G. Qiu, G. Chen, and S. Shu, *Geocryology in China*, Science Press, Beijing, China, 2000.

[2] O. B. Andersland and B. Landanyi, "Frozen Ground Engineering," John wiley & Sons, Inc. and ASCE American Society of Civil Engineering, New York, NY, USA, Second edition, 2004.

[3] Y. Tian, Z. Yang, B. Tai, Y. Li, and Y. Shen, "Damage and mitigation of railway embankment drainage trench in warm permafrost: a case study," *Engineering Geology*, vol. 261, article 105276, 2019.

[4] R. Zhang and Z. Wang, "The progress of the research on the prevention and cure of the irrigation channel frozen injury in the seasonal frozen soil," *Agricultural Research in the Arid Areas*, vol. 25, no. 3, pp. 236–240, 2007.

[5] Y. Liao, J. Liu, and S. Chen, "Research progress of damage mechanism of frost heave and anti-frost technique of concrete canal," *Rock and Soil Mechanics*, vol. 29, no. S1, pp. 211–214, 2008.

[6] S. Li, M. Zhang, Y. Tian, W. Pei, and H. Zhong, "Experimental and numerical investigations on frost damage mechanism of a canal in cold regions," *Cold Regions Science and Technology*, vol. 116, pp. 1–11, 2015.

[7] P. He, J. Dong, X. Ren, and X. Wu, "Longitudinal deformation model and parameter analysis of canal lining under nonuniform frost heave," *Advances in Materials Science and Engineering*, vol. 2021, Article ID 5519035, 14 pages, 2021.

[8] G. Yang, *Frost Heaving Characteristics and Frost Resistance Measures of Buildings in Seasonal Frozen Soil Area*, Dalian University of Technology, Dalian, Liaoning, China, 2005.

[9] T. Chen, *Establishment and Application of Mechanics Model of Frost Heaving Damage of Concrete Lining Open Canal*, Northwest A & F University, Xi'an, Shaanxi, China, 2004.

[10] G. Jian, "Effects of water on frost damage of canal lining and ways for damage control in north chine," *Technique of Seepage Control*, vol. 2, no. 1, pp. 6–11, 1996.

[11] Z. Y. Cai, H. Chen, Y. H. Huang, and C. Zhang, "Failure mechanism of canal slopes of expansive soils considering action of wetting-drying cycles," *Chinese Journal of Geotechnical and Engineering*, vol. 41, no. 11, pp. 1977–1982, 2019.

[12] P. He and W. Ma, "Study of canals in cold regions of China: achievements and prospects," *Journal of Glaciology and Geocryology*, vol. 42, no. 1, pp. 182–194, 2020.

[13] Z. Wang, "Establishment and application of mechanics models of frost heaving damage of concrete lining trapezoidal open canal," *Transactions of the CSAE*, vol. 20, no. 3, pp. 24–29, 2004.

[14] W. Zhengzhong, L. Jialin, and C. Tao, "Mechanics models of frost-heaving damage of concrete lining trapezoidal canal with arc-bottom," *Transactions of the CSAE*, vol. 24, no. 1, pp. 18–23, 2008.

[15] Y. Wang, Z. Z. Wang, Q. Liu, and M. Xiao, "Experimental investigations on frost damage of canals caused by interaction between frozen soils and linings in cold regions," *Chinese Journal of Geotechnical Engineering*, vol. 40, no. 10, pp. 1799–1808, 2018.

[16] M. Xiao, Z. Wang, Q. Liu, Y. Wang, J. Ge, and X. Wang, "Mechanical model for frost heave damage of large-sized canal considering bi-directional frost heave of frozen soil and lining plate frozen shrinkage," *Transactions of the Chinese Society of Agricultural Engineering*, vol. 34, no. 8, pp. 100–108, 2018.

[17] E. Penner and W. Irwin, "Adfreezing of leda clay to anchored footing columns," *Canadian Geotechnical Journal*, vol. 6, no. 3, pp. 327–337, 1969.

[18] G. Bondarenko and A. Sadovskii, "Strength and deformability of frozen soil in contact with rock," *Soil Mechanics & Foundation Engineering*, vol. 12, no. 3, pp. 174–178, 1975.

[19] K. Biggar and D. Sego, "The strength and deformation behaviour of model adfreeze and grouted piles in saline frozen soils," *Canadian Geotechnical Journal*, vol. 30, no. 2, pp. 319–337, 1993.

[20] B. Ladanyi, "Frozen soil – structure interfaces," *Studies in Applied Mechanics*, vol. 42, no. 6, pp. 3–33, 1995.

[21] Y. J. Ji, K. Jia, Q. H. Yu, H. J. Jin, L. Guo, and X. X. Luo, "Direct shear tests of freezing strength at the interface between cast-in-situ concrete and frozen soil," *Journal of Glaciology and Geocryology*, vol. 39, no. 1, pp. 86–91, 2017.

[22] Z. Wen, Q. Yu, W. Ma et al., "Experimental investigation on the effect of fiberglass reinforced plastic cover on adfreeze bond strength," *Cold Regions Science and Technology*, vol. 131, pp. 108–115, 2016.

[23] T. Chen, G. Zhao, and T. Zhao, "Experimental study on the freezing strength characteristic of clay-structure Interface in cold regions," *China Earthquake Engineering Journal*, vol. 40, no. 3, pp. 512–518, 2018.

[24] Q. B. Shi, P. Yang, and J. Z. Tang, "Development of measuring system by pile-pressing method and experimental study on adfreezing strength at interface between frozen soil and structure," *Chinese Journal of Geotechnical Engineering*, vol. 41, no. 1, pp. 139–147, 2019.

[25] H. Sun, P. Yang, and G. Wang, "Development of mechanical experimental system for interface layer between frozen soil and structure and its application," *Rock and Soil Mechanics*, vol. 35, no. 12, pp. 3636–3641, 2014.

[26] H. Sun, P. Yang, and G. Wang, "Monotonic shear mechanical characteristics and affecting factors of interface layers between frozen soil and structure," *Transactions of the Chinese Society of Agricultural Engineering*, vol. 31, no. 9, pp. 57–62, 2015.

[27] T. L. Wang, H. H. Wang, T. F. Hu, and H. F. Song, "Experimental study on the mechanical properties of soil-structure interface under frozen conditions using an improved roughness algorithm," *Cold Regions Science and Technology*, vol. 158, pp. 62–68, 2019.

[28] SAMR (State Administration for Market Regulation), *Standard for Engineering Classification of Soil*, China Planning Presss, Beijing, 2007.

[29] Z. Zhou, W. Ma, S. Zhang, Y. Mu, and G. Li, "Effect of freeze-thaw cycles in mechanical behaviors of frozen loess," *Cold Regions Science and Technology*, vol. 146, pp. 9–18, 2018.

[30] P. He, Y. Mu, Z. Yang, W. Ma, J. Dong, and Y. Huang, "Freeze-thaw cycling impact on the shear behavior of frozen soil-concrete interface," *Cold Regions Science and Technology*, vol. 173, article 103024, 2020.

[31] P. He, W. Ma, Y. Mu, J. Dong, and Y. Huang, "Study on freezing strength characteristics and formation mechanism of frozen soil-concrete interface," *Transactions of the Chinese Society of Agricultural Engineering*, vol. 34, no. 23, pp. 127–133, 2018.

[32] T. F. Hu, J. K. Liu, and J. H. Fang, "Experimental study on the effect of cyclic freezing-thawing on mechanical properties of silty clay with different degrees of compaction," *Chinese Journal of Rock Mechanics and Engineering*, vol. 36, pp. 1495–1503, 2017.

[33] M. X. Gao, X. F. Li, and W. J. Liu, "Influence on compactness and water content to frozen soil properties," *Journal of Inner Mongolia Agricultural University*, vol. 33, no. 3, pp. 186–189, 2012.

[34] X. Zhu, G. Q. Li, Z. Y. Cai, Y. H. Huang, C. Zhang, and H. Chen, "Failure modes and slope stability of expansive soil canal under wet-dry cycles," *Transactions of the Chinese Society of Agricultural Engineering*, vol. 36, no. 4, pp. 159–167, 2020.

[35] Z. Zhou, W. Ma, S. Zhang, Y. Mu, and G. Li, "Experimental investigation of the path-dependent strength and deformation behaviours of frozen loess," *Engineering Geology*, vol. 265, article 105449, 2020.